

# 1 Optimization of a Hybrid Community District Heating System integrated with Thermal 2 Energy Storage system

3 Behrang Talebi<sup>1</sup>, Fariborz Haghighat<sup>1\*</sup>, Paul Tuohy<sup>2</sup>, Parham A. Mirzaei<sup>3</sup>

4 <sup>1</sup> Department of Building, Civil and Environmental Engineering, Concordia University,  
5 Montreal Canada, H3G 1M8

6 <sup>2</sup> Mechanical and Aerospace Engineering, University of Strathclyde, UK

7 <sup>3</sup> Department of Architecture and Built Environment, University of Nottingham, UK  
8

## 9 Abstract

10 Evidence from a various research suggests that buildings hold a vital role in climate change by  
11 significantly contributing to the global energy consumption and the emission of greenhouse  
12 gases. Considering the trend of higher energy consumption in the building sector, it is important  
13 to influence this sector by decreasing its energy demand. District generation and cogeneration  
14 systems integrated with the energy storage system have been suggested as a potential solution  
15 to achieve such planned goals.

16 Unlike the older generation of the DHS, where the focus of the design was on minimizing the  
17 system heat loss, in 4<sup>th</sup> generation DHS, achieving higher system efficiency is made possible  
18 by picking the optimal equipment size as well as adopting the appropriate control strategy.

19 Designers have adopted different design methods for selecting the equipment size, however,  
20 finding the optimal size is a challenging task. This paper reports the development of a simplified  
21 methodology (dynamic optimization) for a hybrid community-district heating system (H-  
22 CDHS) integrated with a thermal energy storage system by coupling the simulation and  
23 optimization tools together. Two, existing and newly built communities, have been considered  
24 and the results of the optimization on the equipment size of both communities have been  
25 studied. The results for the newly built community is later compared with the one obtained from  
26 the conventional equipment size methods whereas static optimization methods and potential  
27 size reduction with the conventional method has been obtained.

28 **Keywords:** Hybrid Community-District Heating System; Thermal Storage; Multi-Objective  
29 Dynamic Optimization; Load Prediction Method

30 \*Corresponding Author: [Fariborz.Haghighat@Concordia.ca](mailto:Fariborz.Haghighat@Concordia.ca)  
31  
32  
33

<i>Variable</i>	<i>Description</i>	<i>Unit</i>
$A$	Thermal Storage Exterior Area	$m^2$
$C$	Cost	£
$Cap_{TS}$	Capacity of Thermal Storage	$m^3$
$CP_{wt.}$	Specific Heat of the Fluid, Water	$kJ/kg.K$
$E$	CO <sub>2</sub> Generation	$kg \text{ of } CO_2$
$E_{n,m}$	Equivalent Emission Generated by Boiler $n$ at Year $m$ per Unit of Energy Generated	$kg.CO_2/kg.fuel$
$ExCap_m$	Extra Capacity of Boiler $m$	$kW$
$FC_{n,m}$	Fuel Cost of Boiler $n$ at Year $m$	£
$i$	Annual Interest Rate	%
$IC$	Initial Cost	£
$IC_m$	Base Cost of the Boiler $m$	£
$IE_{Aux.}$	Equivalent Emission Generated by Imported Energy Year $m$ per Unit of Energy Generated	$kg.CO_2/kg.fuel$
$IN$	Annual Income from Selling Energy to Off-Site	£
$LC_m$	Linearized Cost of Boiler $m$	£/kW
$LC_{TS}$	Linearized Cost of Thermal Storage	£/m <sup>3</sup>
$Loop_{DN}$	Demand Side Loop	$kWh$
$M$	Boiler Number	
$N$	Year Number	
$\square_{Ch.}$	Charging Efficiency = 0.98	
$\square_{Dis.Ch.}$	Discharging Efficiency = 0.96	
$OC_{annual}$	Annual Operational Cost	£
$PRFF_n$	Primary Resource Factor of the Fuel	
$PRFIE$	Primary Resource Factor of the Imported Fuel	
$PW_{oc}$	Present Worth of Operational Cost	£
$Q_{BLDG(t)}$	Energy Required by the Buildings, Users, at Time $t$	$kWh$
$Q_{Gen(t,n)}$	Energy Generated by Boiler $n$ at Time $t$	$kWh$
$Q_{Losses(t)}$	Energy Lost Through Distribution Network at Time $t$	$kWh$
$Q_{Net(t)}$	Net Energy Required by the Network at Time $t$	$kWh$
$Q_{TSCh(t)}$	Energy Sent to Thermal Storage at Time $t$	$kWh$
$Q_{TSDis.Ch(t)}$	Energy Discharged From Thermal Storage at Time $t$	$kWh$
$Q_{TS.loss(t)}$	Energy Loss of the Thermal Storage at Time $t$	$kWh$
$T_{OA(t)}$	Outdoor Temp. at Time $t$	°C
$T_{TS(t)}$	Thermal Storage Temp. at Time $t$	°C
$U$	Overall Heat Transfer Coefficient of Thermal Storage	$W/(m^2.K)$
$V$	Volume of the Thermal Storage	$m^3$
$V_{Aux.}$	Amount of Imported Fuel Used to Generate a kWh of Energy	$kg.fuel/kWh$
$V_{n,m}$	Amount of Fuel Used to Generate a kWh of Energy	$kg.fuel/kWh$
$\rho_{wt.}$	Density of the Fluid, Water	$kg/m^3$

35

36

37

38

39

40

## Abbreviation

Abbreviation	Description
H-CDHS	Hybrid Community District Heating System
DHS	District Heating System
DHW	Domestic Hot Water
NTHU	Non-Typical High Usage
NTMU	Non-Typical Medium Usage
NTLU	Non-Typical Low Usage
TTCU	Typical Thermostat Control Usage
TMY	Typical Meteorological Year
MLCP	Mixed Linear Complementarity Programing
LCC	Life Cycle Cost

41

42

43

## Major TRNSYS Components

Type No.	Name	Representing
700	Simple Boiler with Efficiency Input (Modified)	<i>Biomass Boiler</i>
659	Auxiliary Fluid Heater with Proportional Control (Proportional Boiler)	<i>Auxiliary Boiler</i>
.	Equa. 2	<i>Boiler House Controller</i>
.	Equa. 3	<i>Network Controller</i>
534	Vertically Cylindrical Storage Tank with Optional Immersed Heat Exchanger	<i>Thermal Storage</i>
512	Sensible Heat Exchanger With Hot-Side Modulation	
940	Tank-less Water Heater	
977	Variable Speed Pump	<i>Circulation Pump</i>
604a	Bi-Directional, Noded Pipe with Wall & Insulation Mass	
952	Buried Single Pipe	<i>Under Ground Distribution Network</i>
682	Load Imposed on a Liquid Stream	

44

45

46

47

48

49

50

51

52

53

## 54 1. Introduction

55 As a major energy consumer, the building sector accounts for about 40% of the total  
56 energy consumption in North America and Europe, respectively [1]. Various countries  
57 prioritize the implementation of energy enhancement strategies in this sector to respect the Paris  
58 Climate Accord, COP21[2]. Such strategies have been applied at various levels, including  
59 energy production, conversion, and user-demand, but the most effective solution touches the  
60 higher level known as energy management [3].

61 A Hybrid<sup>1</sup> Community-District Heating System (H-CDHS) is a unique type of energy  
62 management integrating thermal storage within its multi-source energy fed system. Two types  
63 of renewable sources exist in terms of availability a) intermittent sources such as wind and  
64 solar, and b) non-intermittent sources such as biomass and geothermal. For the intermittent  
65 sources, thermal storage can regulate the demand which could decrease the dependency on non-  
66 renewable sources. However, for non-intermittent sources, thermal storage can appreciably  
67 improve the system performance and its efficiency in other ways such as peak demand shaving.  
68 [4].

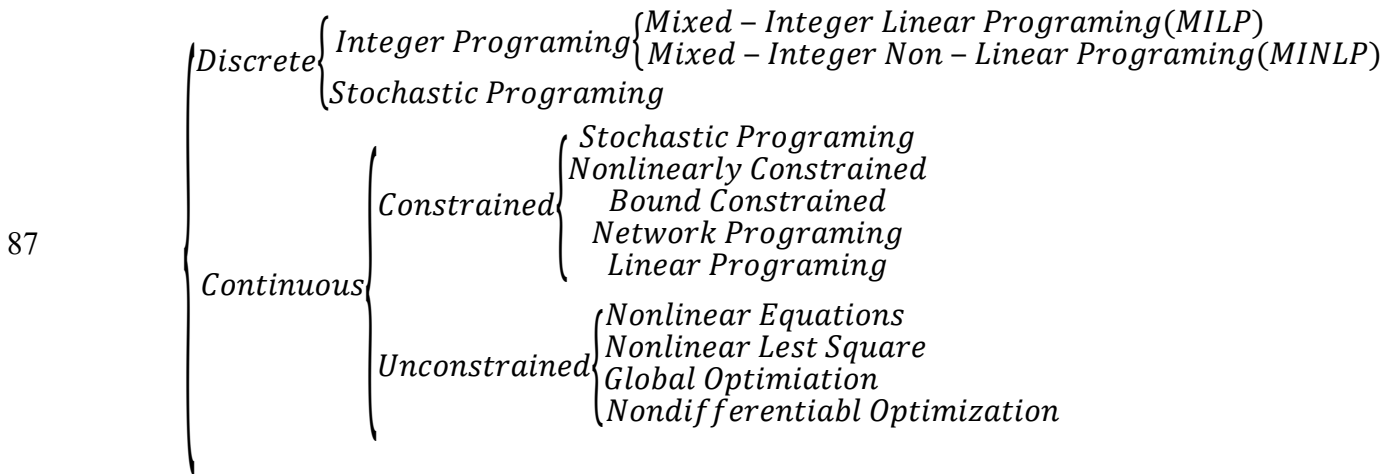
69 The major design issue of the older district heating system (DHS) generations (1<sup>st</sup> to 3<sup>rd</sup>  
70 generation) was mainly high heat loss in the distribution network due to the high-temperature  
71 media (100°C and more) [5, 6]. In this regard, the optimization focus was on enhancing the  
72 system efficiency by controlling the heat loss from the system and subsequently, improving the  
73 system efficiency. As a result, most optimization studies have focused on minimizing the  
74 system heat loss. However, the new generation DHS (4<sup>th</sup> generation) operates at a lower  
75 temperature (50-60°C), and hence achieving higher system efficiency is possible by adopting

---

<sup>1</sup> The term hybrid, represent the use of multiple energy generation sources, renewable source (Biomass Boiler) and non-renewable source (Gas Boiler), used in the boiler house.

76 appropriate control strategies and also through optimization of the equipment size [7, 8]. Note  
 77 that, designing the 4<sup>th</sup> generation DHS based on the conventional design method, sizing the  
 78 equipment based on the peak demand load, could lead to oversizing of the equipment and low  
 79 system efficiency. Therefore, the adoption of an optimal approach (for cost, energy and  
 80 environmental impact) to enhance the efficiency of the DHS while designing the 4<sup>th</sup> generation  
 81 DHS became a standard practice among designers.

82 Different optimization methods have been developed to improve H-CDHS efficiency  
 83 and to reduce the system's emission footprint and the overall cost [4, 9]. Among the existing  
 84 methods, mathematical methods based on continuous or discrete variables (**Figure 1**) [3, 10-  
 85 12], generic algorithms [3, 13-15] and neural networks systems are the most implemented  
 86 techniques for optimizing the DHS efficiency.



88 **Figure 1:** Summary of mathematical based optimization approaches

89 **1.1. Static and Dynamic Optimization**

90  
 91 Besides the mathematical approaches (as shown in **Figure 1**) adopted to formulate the  
 92 optimization process, the optimization methods could be categorized either as static or dynamic  
 93 optimization based on the dependency of the decision-making process with respect to time. In

94 static optimization, the optimization time period remains the same for each iteration and the  
95 optimal solution is selected for a particular point of time within the given time period. In other  
96 words, in each iteration, regardless of any change in the optimization variables, the optimal  
97 solution is always at the same time. For example, static optimization obtains the optimal size  
98 of the equipment based only on the annual peak demand load. While in dynamic optimization,  
99 the optimization time horizon is split into a set of smaller time periods and the solution for each  
100 period affects the future solutions and possibilities. As a result, the optimizing agent takes into  
101 account this effect in the decision-making process.

102           Even though there is a scientific consensus on the mathematical definition of the static  
103 and dynamic optimization processes, there are many ongoing debates as to which type of  
104 optimization method should be used when it comes to use of the commercial energy simulation  
105 and optimization tools. Since similar simulation output could be obtained from all these  
106 commercial methods (e.g. energy demand profile), the interaction between the simulation and  
107 optimization tools can be used to identify the optimization type (static or dynamic  
108 optimization). For instance, in static optimization, the district component and the interaction  
109 between them are modeled either using the user-defined code or commercial simulation  
110 software [19, 20] in order to find the optimal size of the DHSs' equipment [11, 16-18].  
111 Subsequently, the energy simulation is performed exclusively from the optimization process  
112 and a set of unique solution is obtained per simulation. In other words, the optimization  
113 population is generated by simulating the model over the simulation time period under different  
114 scenarios (optimizations variables) and the unique solution is obtained based on the objective  
115 function (i.e. cost and emission) under each scenario. Later on, the optimization tools use the  
116 unique solutions as an optimization population to find the optimized value of the objective  
117 function. It is worth mentioning that all unique solutions obtained from static optimization are  
118 for the same exact point of time (e.g. the peak demand time). By using the non-interactive

119 model, i.e., separate simulation and optimization model (static model), there exists a higher  
120 probability of decreasing the effectiveness of the optimization tool towards predicting the  
121 optimal size of the equipment [16].

122 On the other hand, in dynamic optimization, instead of generating the optimization  
123 population by simulating the model for different scenarios, the optimization and simulation are  
124 carried out simultaneously. By simultaneously performing the optimization and simulation, not  
125 only a more comprehensive spectrum of the solution is generated as an optimization population,  
126 but also the generated off-spring population reflect the effects of previous hours. Due to the  
127 complexity of coupling the simulation and optimization tool in dynamic optimization, several  
128 research works focused on the dynamic optimization using user-defined codes for system  
129 modeling<sup>2</sup> [12, 21-23].

130 Since the dynamic optimization of the system using the detailed user-defined codes is  
131 computationally expensive, and in many cases not feasible, different simplification approaches  
132 have been adopted to decrease the computational time. These approaches resulted in a  
133 simplification of the district energy model<sup>3</sup>, using the reduced input file and the representative  
134 weather or demand file for the design period instead of using the whole year profile, or the  
135 combination of two. Considering the above-said research gap, the main objective of this study  
136 is to develop a dynamic optimization platform that could explore the optimal equipment size  
137 using the detailed demand profile in a timely manner. The developed model predicts the detailed  
138 demand profile of the DHS and uses them along with detailed energy model of the DHS and  
139 the equipment, and the interaction between them to dynamically optimize the entire system.  
140 Subsequently, the optimal size of the equipment is obtained. The size of the equipment obtained

---

<sup>2</sup> Modeling the district components and the interaction between them.

<sup>3</sup> Represent the components and the interaction between them with a simplified equation

141 from the model is later compared with the one obtained from the conventional method (design  
142 day method), as well as using a static optimization tool, (Biomass optimization tool). In this  
143 regard, data from an existing H-CDHS with an integrated thermal energy storage system is used  
144 to optimize its boiler house to minimize its overall cost and CO<sub>2</sub> emission.

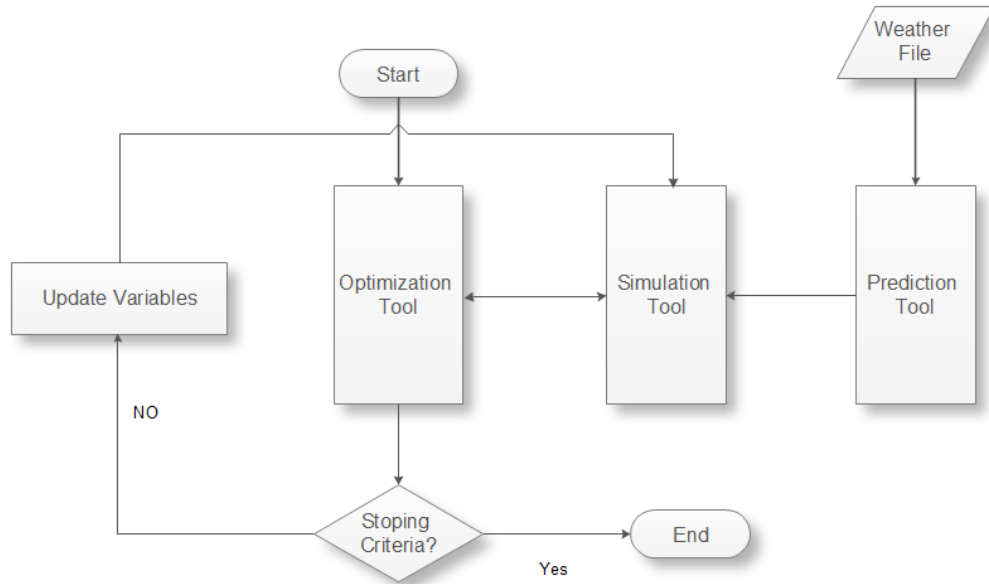
145

## 146 2. Methodology

147 In this study, a mid-size H-CDHS considered earlier was used [24, 26]. The selected  
148 community is located in Cambuslang, Scotland and consists of 3 different types of residential  
149 buildings, newly renovated towers, newly built duplex detached houses and 4-story terrace  
150 buildings, with a total of 640+ units. Multiple energy sources such as gas and wood pellets were  
151 used to provide the required energy to meet the heating and DHW demands. A well-insulated  
152 underground pipe network with a total length of 6 km (supply and return) is used to distribute  
153 the energy between the generation and consumers. TRNSYS was used as the simulation  
154 platform to define the relationship between various system components and to couple the  
155 prediction and optimization tools. Also, a previously developed simplified load prediction  
156 model by the authors was used to dynamically predict the system demand load [24] . Results  
157 obtained from the prediction tool (User Code) demand profile of the system, were fed as input  
158 to the TRNSYS file in the text format. Adopting the predicted demand profile, TRNSYS model  
159 determines the load required to be generated by the boiler house or to be stored in the thermal  
160 storage by comparing the available stored energy and the predicted demand load.. Knowing the  
161 net demand profile and the partial efficiency profile of each boiler, TRNSYS determines the  
162 type and amount of the fuel required to offset the remaining demand. In the next step, the type  
163 and amount of fuel as well required size of boilers and thermal storage are sent to the  
164 optimization tool (GenOpt.) in form of an input file. Considering all the different possibilities,



165 the optimization tool determines the optimal size of the equipment and overwrites the  
166 equipment size in the simulation tool, [Figure 2](#).



167

168 **Figure 2:** Prediction, Simulation, and Optimization Process Flowchart

### 169 2.1. Load Prediction

170 To optimize an H-CDHS, the first step is to predict the hourly energy demand profile of  
171 the entire H-CDHS, which includes the energy consumption and its corresponding losses. In  
172 general, there are three different techniques to obtain a community's energy demand profile:  
173 direct measurement, a comprehensive energy simulation tool used when data is not available,  
174 and simplified prediction methods in cases with high computational costs.

175 In this study, a simplified four-step procedure developed was used to predict the  
176 communities' energy demand profile [26]. The proposed model, by studying the energy  
177 behavior of the users, first, cluster the users into different groups, based on their energy  
178 consumption behavior. After segmenting the units among different clusters, the reference  
179 building for each cluster was obtained. In third step, using the energy consumption behavior of  
180 the reference building, the MLR model for each cluster was trained and used to predict the  
181 energy demand profile of the remaining unit within that cluster. The accuracy of the proposed

182 procedure was validated using two different approaches, using both an inter-model comparison,  
183 and comparing with measured data [26]. Using the validated model, the community demand  
184 profile was predicted for two different scenarios:

- 185 • **Scenario I:** Optimizing the district's existing condition by considering users'  
186 demographic distribution regarding energy consumption habits.
- 187 • **Scenario II:** Optimizing the community as a newly built district by using design  
188 criteria and thermostat control to simulate all users' energy behavior.

189 Before performing the above-said optimization scenarios, in the first step, the  
190 community demand profile was predicted. In order to predict the community demand profile,  
191 occupants were divided into four different groups based on their energy consumption habits<sup>4</sup>.  
192 The definition of each group and its contribution to the total population presented in more  
193 detailed in [26]. Once these groups' energy consumption habits were available, the prediction  
194 model was trained using the proportion of each group within the community.

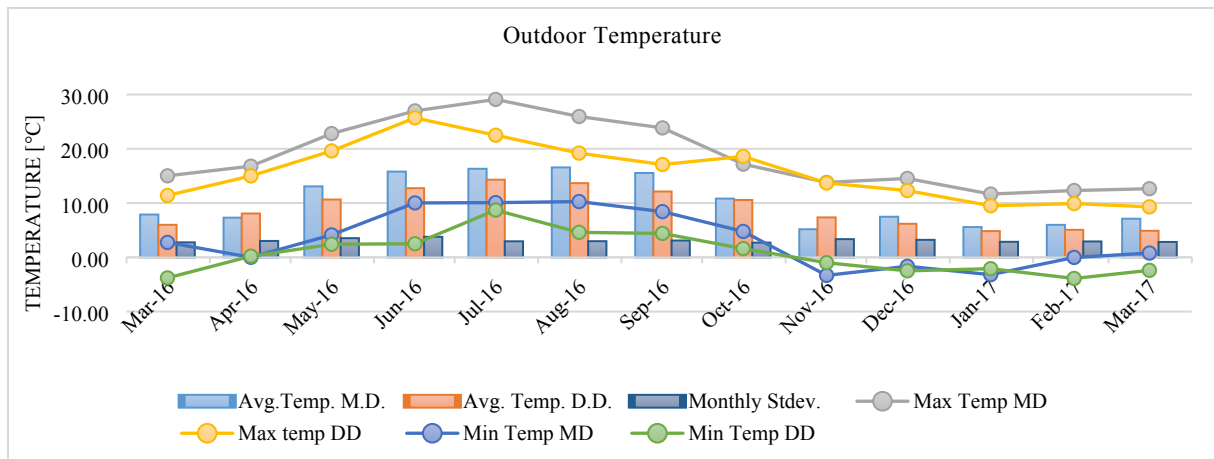
195 In the **Scenario I**, the proportion of the different occupants' type within the community  
196 remained constant and the results served as a basis of comparison for the optimization process.  
197 Leaving occupants' demographic distribution untouched, the district energy demand profile for  
198 **Scenario I** was predicted using the on-site weather data. Then using the on-site measured data  
199 the accuracy of the energy simulation tools' (TRNSYS) was validated, as the all on-site  
200 measured data correspond with this scenario. As a result, **Scenario I** compares the effect of  
201 optimized equipment size and control strategy on energy consumption pattern of the existing  
202 community, its CO<sub>2</sub> emission, and cost.

---

<sup>4</sup>(*Non-Typical High Usage (NTHU)*, *Non-Typical Medium Usage (NTMU)*), *Non-Typical Low Usage (NTLU)* and *Typical Thermostat Control Usage (TTCU)*) [26]

203           Conversely, in *Scenario II*, due to non-availability of data regarding the real time  
204 weather and occupancy condition, both weather file and occupants' demographic distribution  
205 were replaced by the design condition. Hence in this scenario, the TMY3 weather file was used  
206 as a weather input data and, *Typical Thermostat Control Usage* (TTCU) profile was used as an  
207 occupancy profile. Note that the main difference between two scenarios is the energy behavior  
208 of the users. In newly built communities, due to unknown energy consumption profile of the  
209 users, the energy demand profile of the community was obtained based on the predefined  
210 schedules and the minimum temperature mandated by codes. However, in existing  
211 communities, using the same procedure results in over estimating the energy consumption of  
212 the community. In order to compare the effect of difference in energy demand profile on the  
213 equipment size, boiler house under both scenarios has been sized and compared with each other.  
214 As a result, in the first scenario, the existing community was sized by clustering the users and  
215 adopting the actual energy behavior of them. However, in *Scenario II*, equipment has been sized  
216 using the energy behavioral schedules and temperature mandated by codes, and subsequently  
217 the obtained results were compared with the conventional method as well as static optimization  
218 methods. Comparing the TMY3 file with the onsite measured weather data file used for  
219 validating the model shows the average outdoor temperature of 9.3°C and 10.8°C, and the  
220 minimum outdoor temperature of -3.9°C and -3.3 °C for TMY3 and onsite measured data,  
221 respectively. Comparing the TMY3 average and minimum temperature, higher total load and  
222 peak demand load are expected for both scenarios.

223           After obtaining both scenarios' typical usage behavior, a prediction model was trained  
224 based on the fraction of each community group's data. **Figure 3**, shows the design weather  
225 data, TMY3, and onsite measured weather data, while Figure 4 shows the demand heating  
226 profile for these two scenarios.

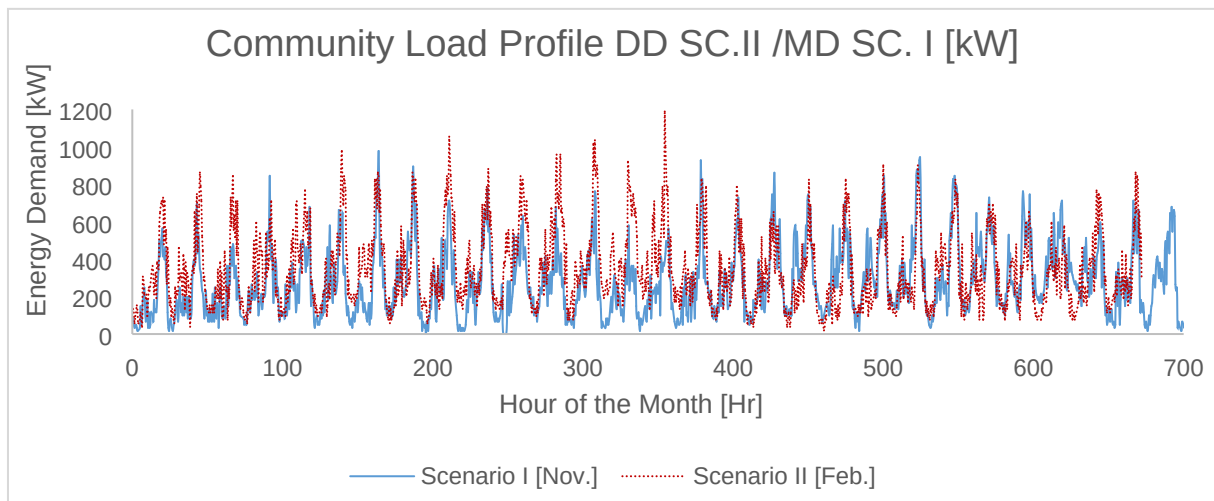


227

228

**Figure 3:** Outdoor weather data (MD: Measured Data and DD: Design Data)

229



230

**Figure 4:** Predicted Demand Profile for *Scenario I* (November) & *Scenario II* (February)

231

232

233

**Figure 4** shows the heating demand profile of *Scenario I & II* for the month when the peak demand load occurred. The inference from the figure is that the peak-heating demand load is 977.3 kW (2.8 % higher compared to the onsite measured data) in the *Scenario I*, and 1189 kW (25.1 % higher compared to the onsite measured data) for *scenario II*. Note that, in *Scenario II*, the entire community was simulated assuming all units were conditioned using the thermostat control (TTCU). It is also important to note that domestic hot water usage was constant for both scenarios. Therefore, the 25.1% increase in peak demand load was associated only with the community's higher heating demand.

240

## 241 2.2. Energy Modelling

242 TRNSYS was used to predict the district energy demand profile and the interaction between its  
243 different components. To represent components, such as biomass boilers and building stock,  
244 existing types in TRNSYS were modified. In general, TRNSYS has three major loops:

### 245 2.2.1. Generation Loop

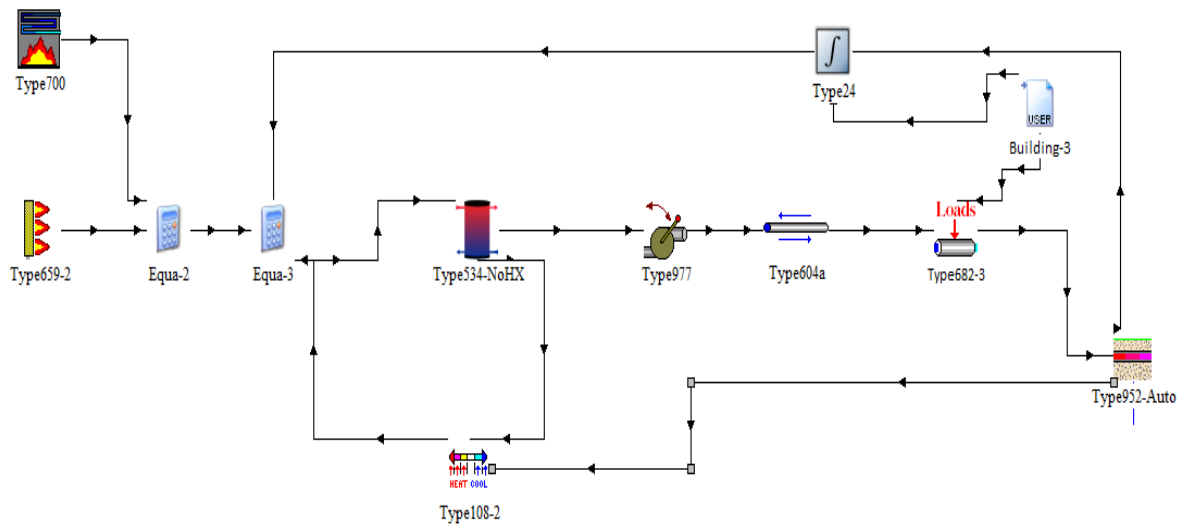
246 The first loop (generation loop) consists of the auxiliary gas, biomass boilers, a  
247 controller, and a heat exchanger, which feeds energy into the system, as shown in **Figure 5** and  
248 **Figure 6**. Since no specific biomass boiler type exists in TRNSYS, *Type 700* was modified to  
249 represent the biomass boiler by adjusting its efficiency, partial efficiency, and the control signal.  
250 After adjusting the boilers' type, two controllers were assigned to the generation loop to adjust  
251 the flow pattern between the generation/consumption loops and the storage loop. The first  
252 controller compared the network's predicted demand load with the total capacity of the boiler  
253 house and the need for the thermal energy storage system as a backup. The second controller  
254 decides which boiler (biomass or gas) should operate to provide the required energy.

### 255 2.2.2. Consumption Loop

256 The consumption loop was constructed with *Type 682*, which represents the demand  
257 profile of all units, (**Figure 4**). This *Type* reads the predicted demand profile through an external  
258 link. The distribution network heat loss was modeled using *Type 952*.

### 259 2.2.3. Storage Loop

260 The storage loop was formed with two different configurations. The first configuration  
261 was modeled by simultaneously charging and discharging the thermal storage as shown in  
262 Figure 5.



263

264

**Figure 5:** Simultaneous charging and discharging configuration

265

266

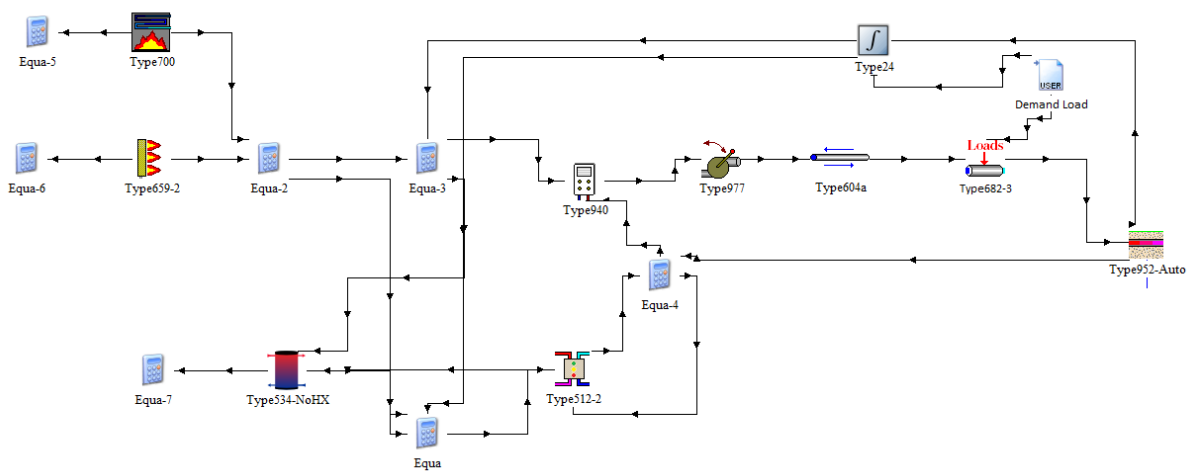
267

268

269

270

In other words, both the boiler house and distribution network was connected to the thermal energy storage system. While the boiler house provided energy to the thermal storage system, the latter supplied the energy to the distribution network. The second configuration was modeled using a step-wise energy storing procedure (Figure 6). In this configuration, a controller monitored the direction to the thermal storage tank (either charged or discharged).



271

272

**Figure 6:** Step-wise charging and discharging configuration

273 By comparing the preliminary results obtained from the total heat loss of the two  
274 configurations (simultaneous and stepwise), it is inferred that the step-wise charging and  
275 discharging configuration had the lower heat loss than simultaneous charging/discharging  
276 configuration due to thermal system storage size and flow direction. Also, the step-wise  
277 charging and discharging configuration has a higher overall energy efficiency compared with  
278 the simultaneous charging/discharging due to on/off frequency of the generation loop in this  
279 configuration (refer [Figure 5](#) & [Figure 6](#)). More detailed explanations regarding the efficiency  
280 of the system are given in the following sections. As a result, the second configuration is used  
281 as a base for optimization.

### 282 **2.3. Optimization Formulation**

283  
284 As mentioned earlier in literature review, the main focus of this study is to optimize the size of  
285 the equipment in a dynamic manner. Existing method, such as using TRNSYS type 56 or Energy plus  
286 optimization function (both using GenOpt.) result in static optimization of the model. In both cases, the  
287 energy simulation is performed exclusively from the optimization process. Subsequently, an  
288 optimization population is generated by simulating the model over the simulation time period under  
289 different scenarios (optimizations variables) and the unique solution is obtained based on the objective  
290 function (i.e. cost and emission) for each scenario. The existing method is effective for optimization of  
291 the component which is not sensitive to previous time steps, such as boilers and earlier generation of the  
292 district system which does not have a thermal storage system. However, for components such as thermal  
293 storage systems which are sensitive to the amount of excessive/lacking energy at previous time steps,  
294 this method cannot result in finding the optimized solution. In this aspect, the existing method has been  
295 modified to perform the dynamic optimization.

296 For the design stage, a dynamic multi-objective optimization method was chosen to size the  
297 main components of the district network boiler house for the two defined scenarios. The model  
298 was based on Mixed Linear Complementarity Problem (MLCP) to minimize the objective

299 functions, life cycle cost (LCC) and CO<sub>2</sub> emission. The optimization analysis focused on the  
 300 on-site heat generation, but the option of purchasing auxiliary heating energy was also  
 301 considered. This is because the primary goal of optimization is to size the main components of  
 302 the boiler house to minimize the investment and operational costs over a thirty-year cycle. To  
 303 account for the effects of short-term load fluctuations on the components' optimal size, the  
 304 optimization was conducted daily with an hourly temporal resolution. To improve model  
 305 accuracy, other input data and model characteristics, including minimum and maximum output  
 306 level constraints, and partial load efficiencies, were defined on an hourly basis. The system  
 307 operational and fuel costs were also considered.

308 A controller type (*Equa.-3* in **Figure 6**) was developed to compare the energy generated  
 309 at each time-step with that in the boiler house (*Equa.-2* in **Figure 6**) in accordance with the  
 310 network demand load (*Type 24*)<sup>5</sup> and flow direction. By comparing the demand load and  
 311 generation capacity, controller fed the network first and then it decides whether to use the  
 312 disparity between generation and demand to charge or discharge the thermal storage system,  
 313 [Equation 1-4](#). This implies that the controller regulates flow direction based on the general heat  
 314 balance equation, while other constraints (such as minimum operative temperature ( $T_{TS(t)}$ ))  
 315 were set for the thermal storage ([Equation 9](#)) to ensure a minimum required temperature for  
 316 DHW usage:

$$317 \quad \sum_{n=1}^N Q_{Gen(t,n)} + Q_{TSCh.(t)} - Q_{TSDis.Ch.(t)} \geq Q_{Net(t)} \quad (1)$$

$$318 \quad Q_{Net(t)} = Q_{BLDG(t)} + Q_{Losses(t)} \quad (2)$$

319 If

$$320 \quad Q_{Gen(t,n)} \geq Q_{Net(t)} \rightarrow \begin{cases} Q_{Net(t)} \rightarrow Loop_{DN(t)} \\ Q_{Gen(t)} - Q_{Net(t)} \rightarrow Q_{TSCh.(t)} \end{cases} \quad (3)$$

321

---

<sup>5</sup> Type 24 is the sum of heat loss of underground pipes obtained from Type 952 and the predicted demand load of the buildings obtained from the simplified method and fed to the TRNSYS model as an external user file (Demand Load)



$$322 \quad Q_{Gen(t,n)} < Q_{Net(t)} \rightarrow \begin{cases} Q_{Gen(t)} \rightarrow Loop_{DN(t)} \\ Q_{TS_{Dis.Ch.}(t)} \rightarrow Q_{Net(t)} - Q_{Gen(t)} \rightarrow Loop_{DN(t)} \end{cases} \quad (4)$$

323

324 The equations used for modeling thermal storage, such as total energy at different time-steps  
325 and boundary conditions applied to it, are as follows:

$$326 \quad Q_{TS(t)} = Q_{TS(t-1)} + Q_{TS_{Ch.}(t)} \cdot \eta_{Ch.} - Q_{TS_{loss}(t)} - \left( \frac{Q_{TS_{Dis.Ch.}(t)}}{\eta_{Dis.Ch.}} \right) \quad (5)$$

$$327 \quad Q_{TS(t)} \geq 0 \quad (6)$$

$$328 \quad Q_{TS_{loss}(t)} = (T_{TS(t)} - T_{OA(t)}) \cdot U \cdot A \quad (7)$$

$$329 \quad T_{TS(t)} = T_{TS(t-1)} - \left( \frac{Q_{TS_{Dis.Ch.}(t)} / \eta_{Dis.Ch.}}{V \cdot C_{p_{wt.}} \cdot \rho_{wt.}} \right) + \left( \frac{Q_{TS_{Ch.}(t)} \cdot \eta_{Ch.}}{V \cdot C_{p_{wt.}} \cdot \rho_{wt.}} \right) \quad (8)$$

$$330 \quad T_{TS(t)} \geq 70^\circ C \quad (9)$$

331 After setting up the controllers, the optimization objective function (Equation 10) was  
332 set up with the aim of optimizing the size of the biomass boiler(s) and thermal storage system,  
333 and minimizing the current net cost and CO<sub>2</sub> emissions:

$$334 \quad Min\{Obj(C, E)\} \quad (10)$$

335 where  $C$  and  $E$  are the cost and emission objectives. To make the objective function linear and  
336 to simplify it from 2D to 1D, the optimization of was performed using the equation below:

$$337 \quad Obj(C, E) = \alpha \cdot C / C_0 + \beta \cdot E / E_0 \quad (11)$$

338 where  $\alpha$  and  $\beta$  are the cost and emission importance factor in the final objective function. These  
339 factors were obtained based on the requirements/needs of the management board. Based on the  
340 discussion with the community management office, the value of  $\alpha$  and  $\beta$  was considered as 0.75  
341 and 0.25, respectively. The cost associated function considers the entire C-DHS initial cost in  
342 addition to the present worth of the life cycle operational cost. To define the initial cost  
343 (Equation 12), the main boiler house equipment was divided into two modular modifiable parts  
344 (boilers and thermal storage system) and fixed non-modifiable equipment (pumps and

345 underground distribution pipelines). Note that, only the modular modifiable equipment cost was  
 346 considered in the initial cost function and the initial cost of fixed non-modifiable equipment  
 347 was excluded, as it remains constant regardless of the size of the modifiable equipment. For  
 348 operational costs (Equation 13), the present fuel cost, the selling price of energy, and the buyout  
 349 price of energy for surrounding houses for a 30-year period were considered using present  
 350 worth method<sup>6</sup>.

$$351 \quad IC = \left( \sum_{m=1}^N (IC_m + LC_m.ExCap_m) \right) + LC_{TS}.Cap_{TS} (12)$$

352 where  $IC$  is the linearized initial cost of the boiler house, ‘ $n$ ’ is the number of years,  $FC$  is the  
 353 fuel costs of different boilers; ‘ $m$ ’ is the boiler number,  $IN$  is the annual income from selling  
 354 heat to off-site users and  $E_{tax}$  is the energy taxes. The initial investment cost includes the fixed  
 355 and proportional variable expenses. The fixed component included the market value of the  
 356 smallest size of the equipment available on the market,  $LC_m$ , while the proportional cost was  
 357 determined by linearizing the extra cost associated with the higher capacity of the equipment,  
 358  $LC_m.ExCap_m$ . Hereafter, in the text,  $IC_m$  and  $LC_m.ExCap_m$  are presented as A and BX,  
 359 respectively.

$$360 \quad OC = \left( \sum_{n=1}^N \sum_{m=1}^M FC_{n,m} (1+i)^{-n} \right) - \left( \sum_{n=1}^N IN (1+i)^{-n} \right) + \left( \sum_{n=1}^N \sum_{m=1}^M E_{tax,n,m} (1+i)^{-n} \right)^7 (13)$$

361 The cost function ( $C$ ) is the summation of the initial and operational cost, (Equation 14).

$$362 \quad C = IC + OC \quad (14)$$

---

<sup>6</sup>  $PW_{OC} = OC_{annual} \cdot \left( \frac{(1+i)^n - 1}{i(1+i)^n} \right)$  where  $i$  and  $n$  are the annual interest rate and year number, respectively, and  $OC_{annual}$  is the annual operation cost.

<sup>7</sup> The energy discount rate ( $i$ ) for Scotland is 0.9%

363 The second objective function is defined to minimize the total CO<sub>2</sub> emission. The  
 364 emission associated function was calculated using the following equation:

$$365 \quad E = \sum_{n=1}^N \sum_{m=1}^M (E_{n,m} \cdot V_{n,m} \cdot PRFE_n + IE_{Aux} \cdot V_{Aux} \cdot PRFIE) \quad (15)$$

366 where  $E_{n,m}$  represents the fuel emissions (kg.CO<sub>2</sub>/kg.fuel) used for each boiler (n) in a year (m) of  
 367 the operation;  $IE_{Aux}$  is the emission of the imported energy fed to the system from outside in  
 368 year, (m,) of the operation (kg CO<sub>2</sub>/kg fuel);  $PRFE_n$  is the primary resource factor of the fuel; and  
 369  $V_{n,m}$  is the fuel volume used in each month ‘m’ by the boiler ‘n’ . While calculating the costs,  
 370 the wood price was discounted in order to take into account the government incentive on the  
 371 price of wood pellets to encourage the small community to use biomass boilers. Note that values  
 372 of the primary energy factor for the wood pellets (PRFE) is 1.26 and for the natural gas (PRFIE)  
 373 is 1.2. [27]

374 To optimize the equipment size and to further minimize the overall costs, CO<sub>2</sub> emissions  
 375 over the life cycle, the first step is to define the price and emissions level for the different type  
 376 of fuel. **Table 1** represents the cost and CO<sub>2</sub> values for wood pellets and natural gas as the main  
 377 fuel type for the chosen district. **Table 2** gives the initial cost of the major equipment.

378 **Table 1:** Energy cost & emission for different fuel types

	Emission [kg CO <sub>2</sub> /kWh]	£/kWh
<b>Wood Pellets</b>	0.039	0.061
<b>Natural Gas</b>	0.203	0.046
<b>Buyout</b>	NA	0.12

379  
380

**Table 2:** Investment costs

	Fixed £ [A]	£/kW [BX]	£/m <sup>3</sup>
<b>Wood Pellets Boiler</b>	125,000	362*	NA
<b>Gas Fired Boiler</b>	132,000	180**	NA
<b>Wood Pellets Storage</b>	NA	NA	670
<b>Thermal Storage</b>	NA	NA	1,100

All costs are presented in A+BX; (refer Equation.12)

Installation and other costs were added separately

\* The linearized part was added after first 250 kW

\*\* The linearized part was added after first 200 kW

### 381 **3. Results**

382 As mentioned in Section 2.1, two different load scenarios were defined and served as a  
383 basis of comparison within existing communities (*Scenario I*) or newly built communities  
384 (*Scenario II*). Using the load demand profile for each scenario, the optimization process was  
385 applied separately, and the equipment's optimal size was determined.

#### 386 **3.1. Scenario I (Existing Community):**

387 The *Scenario I* was defined based on the current situation of the H-CDHS regarding  
388 occupants' behavior. By keeping a similar occupancy distribution to that of a real case one, the  
389 potential annual cost saving and CO<sub>2</sub> emission of the district over its life cycle was determined  
390 using the optimal equipment size and flow control (Table 3).

391

392 **Table 3: Scenario I: Optimization results**

Parameters	Existing Situation	Scenario I
Peak Heating Load (kW)	1100	978
Biomass Boiler (kW)	870	477
Auxiliary Boiler (kW)	1300	609
Thermal Storage (m <sup>3</sup> )	50	16.3
Biomass Boiler Size Compared to the Peak Load (%)	79.1	49
Coverage Percentage by Biomass and Thermal Storage (%)	--	95

393

394 The optimization results for this scenario shows a significant reduction in boiler  
395 capacities (45% for Biomass boiler and 53% for the auxiliary boiler) compared to the existing

396 situation. Considering that only one boiler operates at a time, this fact only achieved by utilizing  
 397 a thermal storage system, which balances the demand and supply heat between the generation  
 398 and consumption loops.

399 Comparing the optimized model results with field measurements show a dramatic drop  
 400 in CO<sub>2</sub> emission (171.9 tons of CO<sub>2</sub> /year or 23%), as well as a considerable reduction in the  
 401 total cost of the system (79,056 £/year or 17.6%). The cost and CO<sub>2</sub> reductions are partially due  
 402 to the lower efficiency of the oversized equipment working at a partial load while other parts  
 403 can be associated to the non-optimal control strategy of the system and missing thermal storage.

404 Since specific weather data and occupants' behavior was considered in the *Scenario I*  
 405 (2016-17), the demand energy load of the community could change anytime based on the  
 406 number of tenants or weather conditions. Consequently, after optimizing the system and  
 407 determining the optimal equipment size, the sensitivity of the design to any change in  
 408 community demand load due to change in the users' demographic distribution was determined.  
 409 To do that, two new cases (*High and Low Usage*) were defined. These newly defined cases  
 410 included a change in the fraction of occupants' types<sup>8</sup> in the community compared with the  
 411 existing condition obtained from clustering results. In the *High Usage Case*, the fraction of  
 412 NTLU and NTMU users dropped, were added to the NTHU and TTCU users to represent a  
 413 higher demand load, see Table 4. In the *Low Usage Case*, the number of NTHU users dropped,  
 414 was added to the lower energy consumers such as NTLU and NTMU, see [Table 4](#).

415 **Table 4:** Fraction of the occupants' types in different scenarios

	<i>Low Usage</i>	<i>Scenario I</i>	<i>High Usage</i>
<i>NTLU</i>	23%	16%	10%
<i>NTMU</i>	39%	24%	15%
<i>NTHU</i>	33%	53%	65%
<i>TTCU</i>	5%	5%	10%
<i>Peak Load (kW)</i>	884	978	1,086

<sup>8</sup> NTLU, NTMU, NTHU, TTCU

416

417 By changing the fraction of occupants, the energy demand profile for newly defined  
 418 cases was predicted and provided as input to the energy model (see [Figure 6](#)). The boiler house  
 419 equipment size remained similar to the *Scenario I*. After modeling these newly defined cases,  
 420 the system performance under new conditions was determined. Comparing the percentage of  
 421 the biomass boiler and thermal storage, which can cover the demand load of the community  
 422 between the *Scenario I* and *High Usage Case* (see [Table 5](#)), shows that in the *High Usage*  
 423 *Case* with 11% higher peak, the percentage coverage time by biomass boiler dropped by 1.1%.

424 Table 5: Performance of the optimized system under new demand profile load

<i>Sensitivity Results</i>			
Parameters	Low Usage	<i>Scenario I</i>	High Usage
Peak Heating Load (kW)	884	978	1086
Biomass Boiler (kW)	477	477	477
Auxiliary Boiler (kW)	609	609	609
Thermal Storage (m <sup>3</sup> )	16.3	16.3	16.3
Biomass Boiler Size Compared to the Peak Load (%)	54	49	44
Coverage Percentage by Biomass and Thermal Storage (%)	97.8	95.0	93.9

425 **3.2. Scenario II (Newly Built Community):**

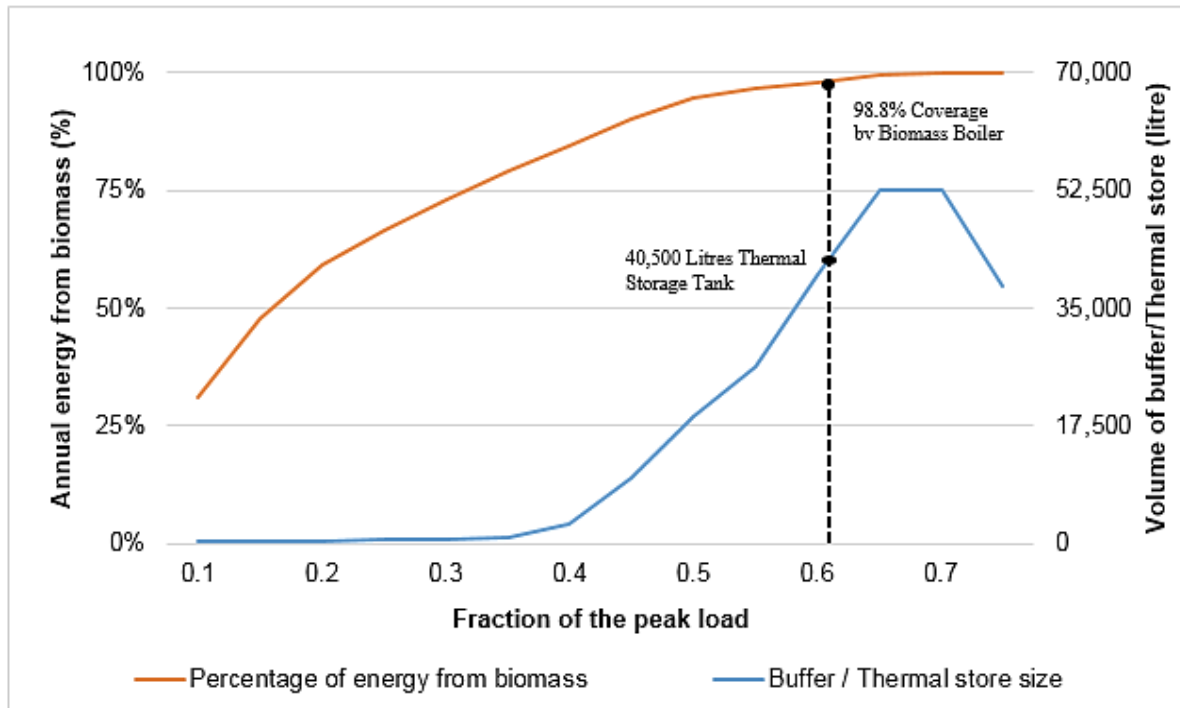
426 In the *Scenario II*, the weather file was changed, and the occupants' distribution was  
 427 altered to the TTCU to represent the design criteria for newly built buildings. [Table 6](#) presents  
 428 the optimal equipment sizes, resulting from the optimization of the boiler house for the  
 429 *Scenario II*.

430 Table 6: *Scenario II*: Optimization results

Parameters	Existing Situation	<i>Scenario II</i>
Peak Heating Load (kW)	1100	1189
Biomass Boiler (kW)	870	661
Auxiliary Boiler (kW)	1300	738

<b>Thermal Storage (m<sup>3</sup>)</b>	50	32.8
<b>Biomass Boiler Size Compared to the Peak Load (%)</b>	79.1	56
<b>Coverage Percentage by Biomass and Thermal Storage (%)</b>	--	98.8

431



432

433

434

**Figure 7:** Optimal Equipment Size, Size of the biomass boiler as a percentage of a peak load for different annual % of energy from a biomass boiler

435

436

437

438

439

440

441

442

443

Similar to the *Scenario I*, the capacity of the boiler optimal size, biomass and auxiliary boiler, used less than 60% of their capacity to respond to the peak demand load. In order to find the optimal size of the equipment using the static optimized sizing tools such as Biomass Boiler Sizing Tool (version 6.8.2), primarily the same annual biomass energy coverage (98.8%) was determined. Using the same coverage percentage, the sizing tool suggests the biomass boiler with the capacity size of 62% of the peak load and 40.5 m<sup>3</sup> thermal storage tank (refer to [Figure 7](#)).

444

Table 7 presents the equipment size and cost associated with each design method.

445



446

**Table 7:** Comparison of the equipment size, cost for different design strategies

Technology	Conventional	Static Optimization Tool		Proposed Dynamic Optimization Process	
		Size	Size Reduction * [%]	Size	Size Reduction * [%]
Biomass Boiler [kW]	870	737	15.3	661	24.0%
Auxiliary Boiler [kW]	1300	891	31.5	738	43.2%
Thermal Storage [m <sup>3</sup> ]	50	40.5	19.0	32.5	35.0%
Cost [£]	734,440	602,224	18.0	538,372	26.7%

447

\* Reductions calculated comparing with conventional method

448

449

450

451

452

453

454

455

456

457

458

459

460

Considering that only one boiler operates at a time, 98.8% coverage by biomass boiler was achieved using only thermal storage to balance between the generation and consumption loop. As shown in [Table 7](#), this solution can reduce the size of both auxiliary and main biomass boilers into a fraction of their original size and, as a result, decrease the system heat loss while improving the district energy efficiency. The reduction in major equipment size of the district using the proposed dynamic optimization method caused a 196,068 £ or 26.7% drop only in the system initial investment cost. Also, knowing the fact that the efficiency of the biomass boiler is lower when operated partially, two scenarios could be assumed for a non-optimal size equipment: 1) the biomass boiler works at its full capacity all the time while keeping the generation efficiency at maximum value; this can result in generation of an excessive amount of heat, which eventually is accounted as loss, and 2) the boiler works at partial load only to meet the network demand. This decreases generation efficiency due to the boilers lower partial capacity efficiency [25]. In both scenarios, the overall efficiency of the system drops.

461

### 3.3. Impact of dynamic optimization in determining the operation period of the system

462

463

464

465

466

467

As mentioned earlier in [Section 1.1](#), the main difference between the static and dynamic optimization is in dependency of the decision-making process with respect to time. In other words, dynamic optimization, by breaking the demand profile into smaller periods and determining a solution for each period, considers the effects of demand at the previous hour on the optimal solution. [Figure 8 \(a\)](#), presents the charging/discharging profile of the thermal

468 storage over the 10 days period in November, obtained from the *Scenario I* and **Figure 8 (b)**  
 469 represents the thermal energy storage mean temperature and the district demand load.

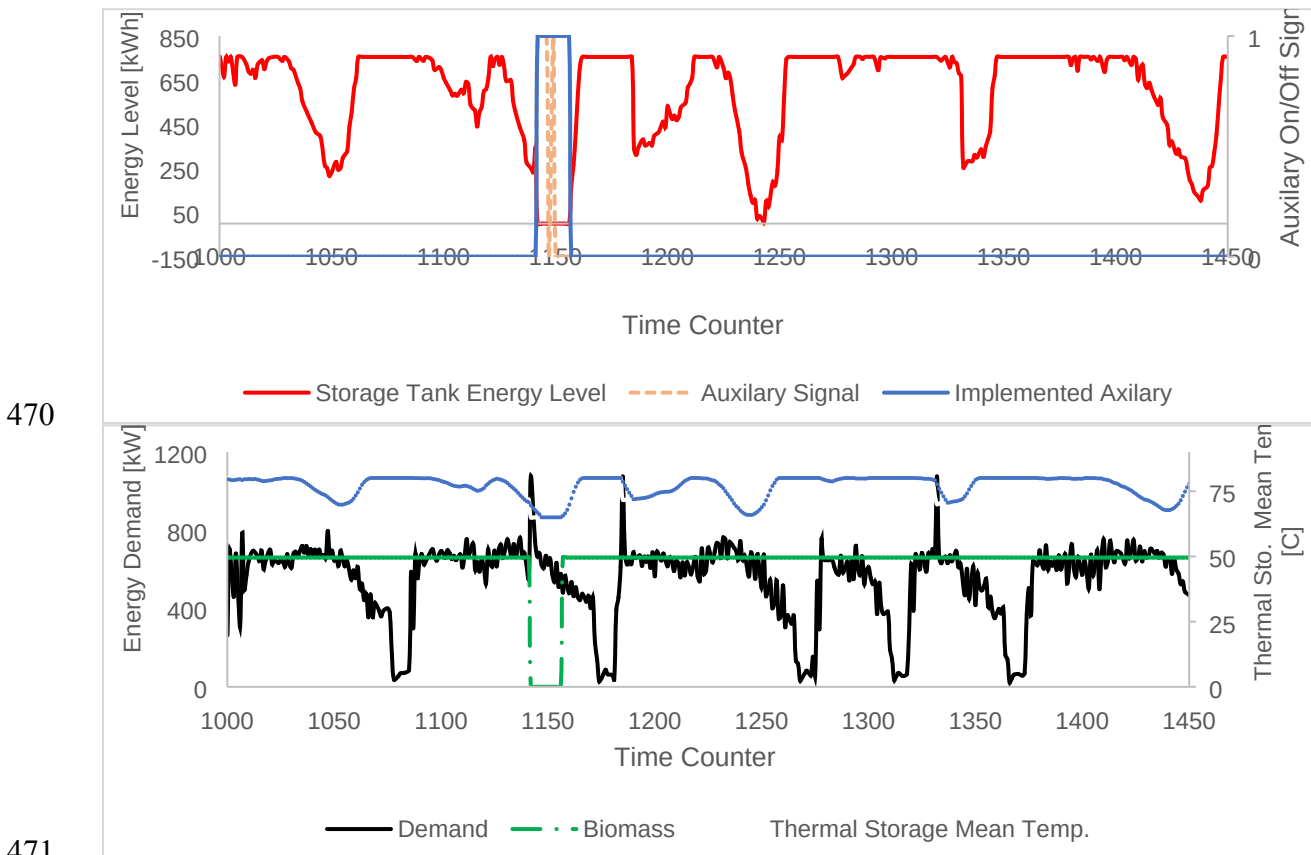


**Figure 8:** (a) Thermal storage energy level for a 10-day period in November; (b) Thermal storage temperature and district demand load for the same 10-days (Bottom)

475 In static optimization by only considering the peak demand in finding the optimal  
 476 solution, the effects of the energy demand at previous hours on determining the optimal solution  
 477 is neglected. On the other hand, in dynamic optimization, by considering the effects of the  
 478 demand profile at a previous hour in determining the optimal solution can result in better  
 479 utilizing of the thermal storage and lower size of the equipment. For instance, as presented in  
 480 **Figure 8**, the response of the system to an identical demand varied based on the energy demand  
 481 of the previous hours. In case of the first peak (shown in **Figure 8 (b)**), due to the high demand  
 482 of the system prior to the peak, the thermal storage has been partially discharged, and as a result,  
 483 the axillary energy is required to respond to the energy demand of the system. On the other

484 hand, due to lower demand of the network prior to the second and third peak, the thermal storage  
485 is fully charged, and no auxiliary energy is required.

486         Apart from determining the optimal size of the equipment, the optimal performance of  
487 the system could be determined from the proposed dynamic optimization method. As shown in  
488 **Figure 8 (b)**, since the biomass boiler works constantly, the district demand load can be met  
489 by a nominal size of the biomass boiler. However, when the demand load of the DHS is higher  
490 than the capacity of the biomass boiler, the deficit energy is met from the thermal energy  
491 storage. On the other hand, when the demand load drops, the surplus energy is stored in the  
492 thermal energy storage and the energy storage level swiftly increases. In peak demand period,  
493 the instantaneous auxiliary system (gas boiler in this case), along with thermal storage, provide  
494 required energy demanded by the district network since the biomass boiler cannot provide  
495 enough energy for the system. Using this strategy while running the biomass boiler constantly  
496 at full capacity for the optimized sized system, step-wise charging/discharging the thermal  
497 storage can eliminate the need for the auxiliary energy 98.8% of the time while maintaining the  
498 system's maximum overall efficiency.

#### 499 **4. Conclusion**

500         This study proposes a novel optimization process called dynamic optimization for  
501 existing and newly built communities by coupling optimization and prediction using a  
502 TRNSYS based energy simulation platform. Optimization performed to calculate the overall  
503 size of major energy generation and storing equipment, and operational control strategy for the  
504 community under different scenarios. In case of the existing community, **Scenario I**, comparing  
505 the optimal equipment size with the existing non-optimal equipment sizes there exists a  
506 considerable difference. The difference in equipment sizes (45% smaller biomass boiler, 53%  
507 smaller auxiliary boiler and finally 67% smaller thermal storage size) between the existing  
508 situation and the **Scenario I** is mainly due to the fact that the existing boiler house has been

509 designed based on the conventional methods. Beside from the drop in the initial cost of the  
510 system (267,716 £ or 38.1%), the annual life cycle cost and CO<sub>2</sub> footprint of the district also  
511 dropped by 79,056 £/year or 17.6% and 171.9 tons of CO<sub>2</sub> /year or 23% respectively. These  
512 drops are due to the higher efficiency of the system operated at full capacity.

513 In case of a newly built district, *Scenario II*, three different design methods have been  
514 used to size the equipment, conventional, static commercial optimization tool, and the  
515 developed dynamic optimization process, and the respective results were compared. The results  
516 indicate that initial cost of the system using the proposed dynamic optimization method could  
517 drop by 26.7% compared with the conventional method while using the static optimization tool  
518 could only result in 18% drop in the initial cost of the system. These facts emphasized the  
519 importance of dynamic optimization of the system in order to achieve the real optimal solution.

## 520 **Acknowledgment**

521 The authors would like to express their gratitude to Concordia University for the support  
522 through the Concordia Research Chair – Energy & Environment.  
523  
524

## 525 **References:**

- 526 1. Chu, S. and A. Majumdar, *Opportunities and challenges for a sustainable energy future*.  
527 Nature, 2012. **488**: p. 294.
- 528 2. Christoff, P., *The promissory note: COP 21 and the Paris Climate Agreement*.  
529 Environmental Politics, 2016. **25**(5): p. 765-787.
- 530 3. Zeng, J., J. Han, and G. Zhang, *Diameter optimization of district heating and cooling*  
531 *piping network based on hourly load*. Applied Thermal Engineering, 2016.  
532 **107**(Supplement C): p. 750-757.
- 533 4. Talebi, B., et al., *A Review of District Heating Systems: Modeling and Optimization*.  
534 Frontiers in Built Environment, 2016. **2**(22).
- 535 5. Wang, W., X. Cheng, and X. Liang, *Optimization modeling of district heating networks*  
536 *and calculation by the Newton method*. Applied Thermal Engineering, 2013. **61**(2): p.  
537 163-170.
- 538 6. Wang, J., Z. Zhou, and J. Zhao, *A method for the steady-state thermal simulation of*  
539 *district heating systems and model parameters calibration*. Energy Conversion and  
540 Management, 2016. **120**: p. 294-305.
- 541 7. Chauhan, A. and R.P. Saini, *Discrete harmony search based size optimization of*  
542 *Integrated Renewable Energy System for remote rural areas of Uttarakhand state in*  
543 *India*. Renewable Energy, 2016. **94**: p. 587-604.

- 544 8. Mehleri, E.D., et al., *A mathematical programming approach for optimal design of*  
545 *distributed energy systems at the neighbourhood level*. Energy, 2012. **44**(1): p. 96-104.
- 546 9. Olsthoorn, D., F. Haghghat, and P.A. Mirzaei, *Integration of storage and renewable*  
547 *energy into district heating systems: A review of modelling and optimization*. Solar  
548 Energy, 2016. **136**: p. 49-64.
- 549 10. Bordin, C., A. Gordini, and D. Vigo, *An optimization approach for district heating*  
550 *strategic network design*. European Journal of Operational Research, 2016. **252**(1): p.  
551 296-307.
- 552 11. Zhou, Z., et al., *Impacts of equipment off-design characteristics on the optimal design*  
553 *and operation of combined cooling, heating and power systems*. Computers & Chemical  
554 Engineering, 2013. **48**(Supplement C): p. 40-47.
- 555 12. Ameri, M. and Z. Besharati, *Optimal design and operation of district heating and*  
556 *cooling networks with CCHP systems in a residential complex*. Energy and Buildings,  
557 2016. **110**(Supplement C): p. 135-148.
- 558 13. Fang, T. and R. Lahdelma, *Genetic optimization of multi-plant heat production in*  
559 *district heating networks*. Applied Energy, 2015. **159**(Supplement C): p. 610-619.
- 560 14. Razani, A.R. and I. Weidlich, *A genetic algorithm technique to optimize the*  
561 *configuration of heat storage in DH networks*. 2016, 2016. **10**: p. 12.
- 562 15. Barberis, S., et al., *Thermo-economic analysis of the energy storage role in a real*  
563 *polygenerative district*. Journal of Energy Storage, 2016. **5**(Supplement C): p. 187-202.
- 564 16. Vesterlund, M., A. Toffolo, and J. Dahl, *Optimization of multi-source complex district*  
565 *heating network, a case study*. Energy, 2017. **126**(Supplement C): p. 53-63.
- 566 17. Wang, H., et al., *Optimization modeling for smart operation of multi-source district*  
567 *heating with distributed variable-speed pumps*. Energy, 2017. **138**(Supplement C): p.  
568 1247-1262.
- 569 18. Rivarolo, M., et al., *Design optimisation of smart poly-generation energy districts*  
570 *through a model based approach*. Applied Thermal Engineering, 2016. **99**(Supplement  
571 C): p. 291-301.
- 572 19. Magnier, L. and F. Haghghat, *Multiobjective optimization of building design using*  
573 *TRNSYS simulations, genetic algorithm, and Artificial Neural Network*. Building and  
574 Environment, 2010. **45**(3): p. 739-746.
- 575 20. Asadi, E., et al., *A multi-objective optimization model for building retrofit strategies*  
576 *using TRNSYS simulations, GenOpt and MATLAB*. Building and Environment, 2012.  
577 **56**: p. 370-378.
- 578 21. Campana, P.E., et al., *Optimization of a residential district with special consideration*  
579 *on energy and water reliability*. Applied Energy, 2017. **194**(Supplement C): p. 751-764.
- 580 22. Schweiger, G., et al., *District heating and cooling systems – Framework for Modelica-*  
581 *based simulation and dynamic optimization*. Energy, 2017. **137**(Supplement C): p. 566-  
582 578.
- 583 23. Sameti, M. and F. Haghghat, *Optimization approaches in district heating and cooling*  
584 *thermal network*. Energy and Buildings, 2017. **140**(Supplement C): p. 121-130.
- 585 24. Talebi, B., F. Haghghat, and P.A. Mirzaei, *Simplified model to predict the thermal*  
586 *demand profile of districts*. Energy and Buildings, 2017. **145**: p. 213-225.
- 587 25. Camporeale, S.M., et al., *Part Load Performance and Operating Strategies of a Natural*  
588 *Gas—Biomass Dual Fueled Microturbine for Combined Heat and Power Generation*.  
589 Journal of Engineering for Gas Turbines and Power, 2015. **137**(12): p. 121401-121401-  
590 13.
- 591 26. Talebi, Behrang, et al., *Validation of a community district energy system model using*  
592 *field measured data*, Energy, 2018. **144**: p. 694-706.

593 27. R. Hitchin, U. Kingdom, K. E. Thomsen, and K. B. Wittchen, "Primary Energy Factors  
594 and Members States Energy Regulations," no. 692447, 2010